JOURNAL OF GEOPHYSICAL RESEARCH, VOL. 107, NO. D15, 4268, 10.1029/2001JD000716, 2002

Product analysis of the OH oxidation of isoprene and 1,3-butadiene in the presence of NO

Michele Sprengnether and Kenneth L. Demerjian
State University of New York at Albany, New York, USA

Neil M. Donahue[1] and James G. Anderson
Harvard University, Cambridge, Massachusetts, USA

Received 4 April 2001; revised 2 August 2001; accepted 8 August 2001; published 13 August 2002.

[1] The oxidation mechanisms of isoprene and butadiene initiated by OH in the presence of NO have been explored under "wall-less" flowing conditions, with products observed a few seconds after reaction by infrared spectroscopy. Since only ~1% of alkene is reacted, any secondary chemistry is negligible. The use of reaction modulation spectroscopy permits the accurate measurement of a percent change in high alkene concentration and of 10^{13} molecules/cm^3 concentrations for products. Measured carbonyl species agree with previous studies, while alkyl nitrate yields are consistent with upper values reported in the literature. NO sensitivity studies performed exclude the possibility of competing chemistry. Isoprene is not observed to form 3-methyl furan, indicating that this is not a prompt oxidation product. However, butadiene does form furan. In an auxiliary experiment, peroxy radicals in the second stage of butadiene oxidation are fully converted to peroxynitrates. Average cross sections for integrated peroxynitrate bands are determined from this experiment. *INDEX TERMS:* 0365 Atmospheric Composition and Structure: Troposphere—composition and chemistry; 0317 Atmospheric Composition and Structure: Chemical kinetic and photochemical properties; 0315 Atmospheric Composition and Structure: Biosphere/atmosphere interactions

1. Introduction

[2] Isoprene, 2-methyl-1,3-butadiene, is the most abundantly emitted biogenic hydrocarbon, and its dominant loss mechanism in the atmosphere is reaction with OH [*Guenther et al.*, 1995; *Poisson et al.*, 2000]. Its oxidation plays an important role in regional ozone production under certain conditions [*Biesenthal et al.*, 1997; *Goldan et al.*, 2000; *Starn et al.*, 1998], it can be a major factor in the hydroxyl radical budget [*McKeen et al.*, 1997; *Stevens et al.*, 1997], and it may significantly influence NO_x chemistry in continental regions via formation of alkyl nitrates [*Chen et al.*, 1998]. Most of isoprene's atmospheric impact is set in motion by its oxidation products. Isoprene's first set of oxidation products remain unsaturated and also include three distinct functionalities: the carbonyl, the hydroxycarbonyl, and the hydroxy alkylnitrate. Each of these species has a different atmospheric impact upon ozone production, NO_x chemistry, and the hydroxyl radical budget. Understanding the oxidation mechanism for isoprene is thus a first-order question in tropospheric chemistry, and while it has received substantial experimental attention, major uncertainties remain.

[3] Over 95% of isoprene-OH reaction occurs by OH radical addition to isoprene in four distinct locations at either side of its two double bonds, and the hydrogen atom abstraction pathway comprises less than 5% of the total reaction [*Campuzano-Jost et al.*, 2000]. The four addition sites lead to a broad suite of primary oxidation products. OH addition to the end carbons (positions 1 and 4) is expected to dominate, with current estimates ranging from 60% to 93% of the overall addition reaction [*Jenkin and Hayman*, 1995; *Lei et al.*, 2000; *Paulson and Seinfeld*, 1992; *Stevens et al.*, 2000]. The second step in the oxidation sequence is addition of molecular oxygen to form a total of eight possible peroxy radicals. When OH addition occurs at an end carbon, resonance in the OH-isoprene adduct makes two sites for O_2 addition available. Again, current predictions for fractional yields vary broadly, from 22% to 50% for the 1,4 addition and 78% to 50% for the addition directly across the original double bond [*Jenkin and Hayman*, 1995; *Lei et al.*, 2001; *Paulson and Seinfeld*, 1992]. The peroxy isomers and a full schematic of the oxidation mechanism are provided in Figure 1.

[4] In the presence of high NO the first stage of stable, molecular products are thought to include a total of eight hydroxycarbonyl species, eight alkyl nitrates, methyl vinyl ketone (MVK), methacrolein (MACR), formaldehyde and 3-methyl furan (3MF). While the latter four species have been measured in several previous studies [*Atkinson et al.*, 1989; *Grosjean et al.*, 1993; *Gu et al.*, 1985; *Killus and Whitten*, 1984; *Miyoshi et al.*, 1994; *Paulson et al.*, 1992; *Tuazon and Atkinson*, 1990a], the composition and relative yields of hydroxycarbonyl and alkyl nitrate products are highly uncertain and account for roughly 35% of the total product yield.

[1]Now at Carnegie Mellon University, Pittsburgh, Pennsylvania, USA.

0148-0227/02/2001JD000716

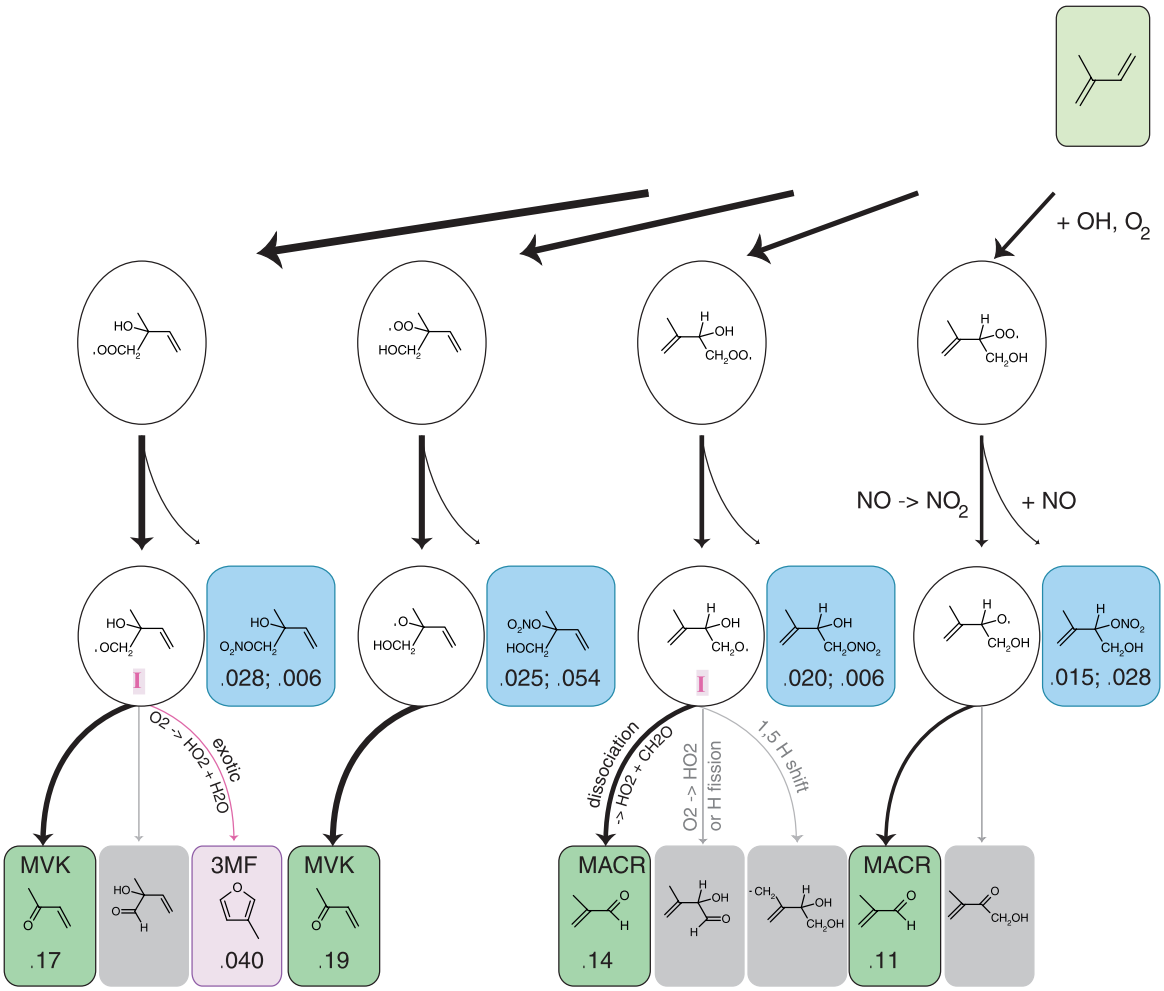

Figure 1. Isoprene oxidation by OH in air with NO.

[5] Although branching ratios have not been directly measured for the first two oxidation steps, OH and O_2 addition, their culmination is constrained by measured MVK and MACR yields. The largest impact of assumed stepwise fractionation is upon relative yields of different alkyl nitrates. *Jenkin and Hayman* [1995] predict 90% addition of OH to end carbons, giving 45% of all alkyl nitrate present as a single isomer, 4-hydroxy-3-methyl-3-

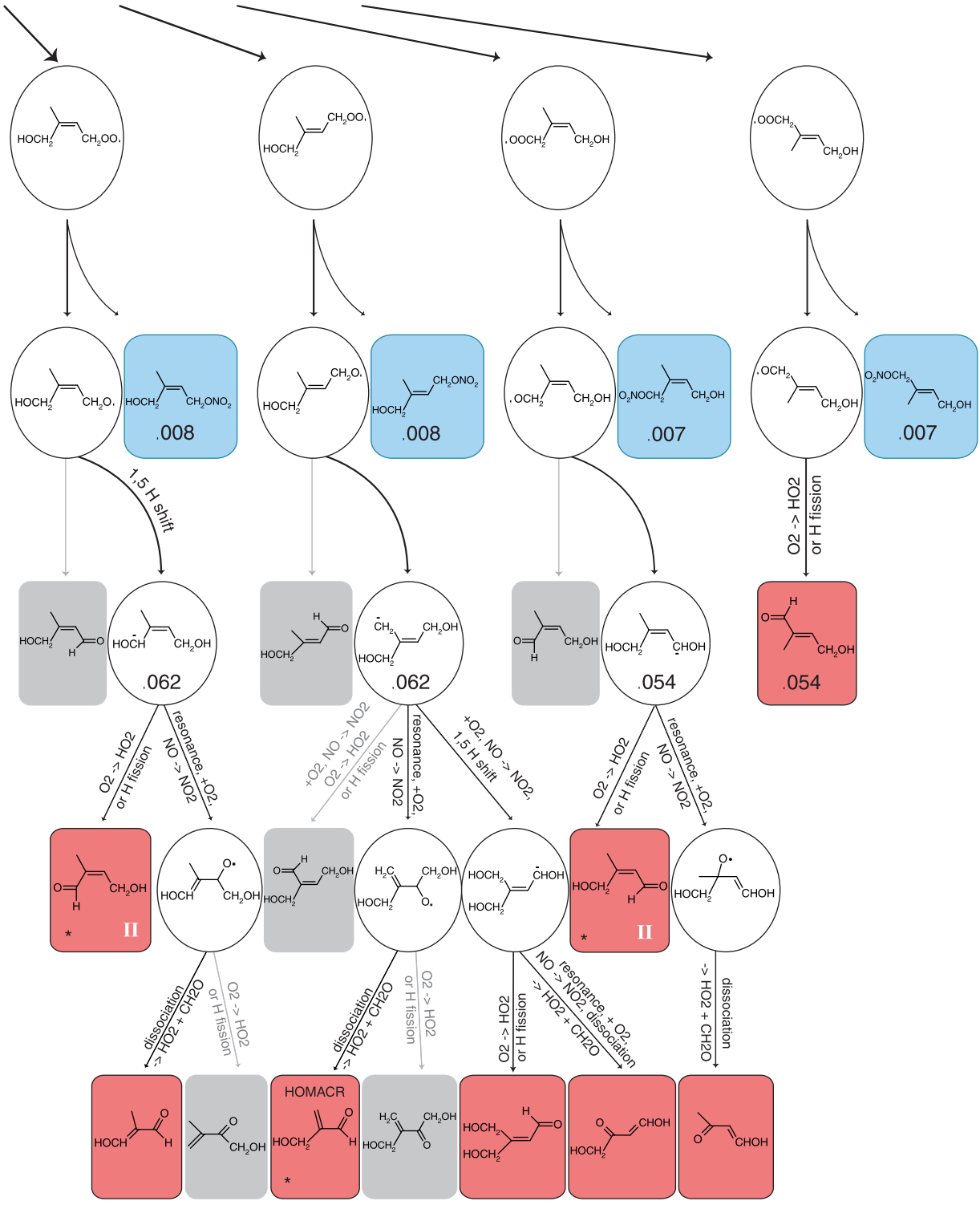

Figure 1. (continued)

nitrooxy-1-butene, while *Paulson and Seinfeld* [1992] predict a more even alkyl nitrate distribution. These predictions assume similar alkyl nitrate fractional yields for each peroxy + NO reaction. A recent experiment [*Chen et al.*, 1998] measures seven separate alkyl nitrate species, with 45–65% of the total nitrate present as a single chromatographic peak, supporting the *Jenkin and Hayman* [1995] mechanism. *Stevens et al.* [2000] recently detected non-negligible mass spectroscopic fragments from each of the four isoprene-OH adducts, supporting a significant contribution from all isomers.

[6] Organic nitrate production is particularly important because it terminates the NO_x-catalysis of atmospheric hydrocarbon oxidation. The recent study of *Chen et al.* [1998] finds a total yield of 4.4% alkyl nitrate that is lower by more than a factor of 2 from previous measurements

[*Tuazon and Atkinson*, 1990a]. Using their lower yields together with Environmental Protection Agency (EPA) emissions estimates, these researchers concluded that up to 7% of NO emitted in the eastern United States during summer months is removed by isoprene's hydroxy nitrate formation. The current uncertainty in this pathway is roughly equivalent to an additional 10% of total NO emissions for this region. The alkyl nitrate yield clearly has important implications on both the ozone-forming potential of isoprene and its impact on regional air quality.

[7] One quarter to one third of all isoprene oxidation by OH is thought to form hydroxycarbonyl products, composed of at least eight separate species, including two sets of three isomers. In contrast to other primary oxidation products of isoprene, methyl vinyl ketone and methacrolein, at least three of these products can form furan rings, and all have a higher solubility. Thus their atmospheric fate and subsequent influence on ozone chemistry can be quite different. However, their reactivity, particularly in solution, together with low individual yields have made their isolation and accurate measurement unattainable.

[8] Attempts to measure hydroxycarbonyl species thus far have been qualitative: C4 and C5 hydroxycarbonyl isomers have been observed by mass spectroscopy [*Kwok et al.*, 1995; *Yu et al.*, 1995]. While *Yu et al.* [1995] observed only a single C5 unsaturated hydroxycarbonyl product, two of the three proposed isomers will readily cyclize in solution and may have done so during the derivatization procedure. A recent product study [*Ruppert and Becker*, 2000] conducted in the absence of NO measured yields for two C5 unsaturated diols, as predicted by analogy to other $RO_2 + RO_2$ reactions.

[9] The asymmetry of isoprene substantially complicates its oxidation mechanism. Consequently, it is important to study 1,3-butadiene as a parallel test system with similar chemistry but with a simpler mechanism. Of note, 1,3-butadiene is a known human carcinogen and toxin that has been measured in U.S. urban areas at 0.14–0.72 ppbv levels, reaching 1-hour concentrations as high as 18 ppbv, similar to very smoky taverns [*U.S. Department of Health and Human Services*, 2001]. Its major source of emission is associated with its industrial use in the manufacture of synthetic rubber, although it is also produced by incomplete combustion in power plants, automotives, forest fires, and cigarette smoke. Previous product studies of 1,3-butadiene oxidation in the presence of NO have measured acrolein as the dominant product, as well as formaldehyde, furan, and generic alkyl nitrates [*Maldotti et al.*, 1980; *Ohta*, 1984; *Tuazon et al.*, 1999]. Again, the missing carbon is thought to comprise hydroxycarbonyls. *Liu et al.* [1999] conducted a smog chamber study and identified several additional carbonyl species, including predicted C4 unsaturated hydroxy carbonyl as well as smaller species produced during subsequent oxidation of first-stage stable products. In addition, a C4 unsaturated carbonyl, glycidaldehyde, a C4 saturated carbonyl, malonaldehyde, a C4 trione, butendial, butadiene monoxide, and butadiene diepoxide were detected. The epoxides may be products from $O(^3P)$ chemistry, while other products may be primary or secondary oxidation products.

[10] A significant shortcoming of previous experiments has been their inability to separate oxidation of the initial reagent (isoprene or butadiene) from oxidation of the subsequent molecular products. This is a general difficulty with environmental chambers, particularly when the product species are as reactive as the parents and have low relative yields, as is true here. The resulting convolution of primary and secondary oxidation products significantly reduces the confidence in derived branching ratios. A second difficulty is the presence of walls: either chamber walls that can serve as a source or sink of radicals, or probe surfaces necessarily introduced in extraction assays such as chromatography or mass spectroscopy. We have previously described a new technique, reaction modulation spectroscopy (RMS), designed to avoid these problems [*Donahue et al.*, 1996a]. The key is to study reactions spectroscopically, in situ, in a wall-less flow system (i.e., diffusion to the wall is too slow to occur during reaction time) under conditions where only a small fraction of the primary reagent is consumed. Periodic modulation (on and off) of the radical source yields very precise difference spectra with noise levels between 1 and 100 ppm fractional absorption. Here we apply RMS to the isoprene and butadiene reactions with OH in the presence of NO. While we have applied this method to perfluoropropene [*Donahue et al.*, 1996a] and cyclopropane [*Clarke et al.*, 1998], this is the first application to highly reactive species of atmospheric importance.

[11] Our focus here is upon the first stage of stable oxidized products: high reactant concentrations with only a small percentage reacting render subsequent reaction negligible. With in situ Fourier transform infrared (FTIR) spectroscopy, we measure MVK, MACR, 3MF, and reacted isoprene, or acrolein, furan, and reacted butadiene, as well as CH_2O, NO, and NO_2 levels for both experiments. In addition, we set upper limits for known products of secondary chemistry and measure total alkyl nitrate yields. An NO sensitivity experiment constrains competing reaction pathways under the present experimental conditions. In an auxiliary experiment we fully convert all peroxy radicals in the second stage of butadiene oxidation to peroxynitrates and report average cross sections for integrated peroxynitrate bands.

2. Experimental Procedure

[12] Experiments were conducted in the Harvard high-pressure flow system which has been previously described in detail (see Figure 2 and *Donahue et al.* [1996a], *Donahue et al.* [1996b], and *Abbatt et al.* [1990]). Isoprene or butadiene was introduced to the carrier flow 8 m upstream of the reaction zone to assure a uniform concentration profile. OH was created using an H_2 microwave discharge followed by subsequent reaction of H with O_2. High levels of HO_2 are expected from this source; however, NO rapidly converts this HO_2 to OH. As isoprene oxidation also produces HO_2, which regenerates OH via NO reaction, many molecules of isoprene are oxidized for each initial H atom. NO is added downstream of the H atom source to minimize formation of NO_2 by NO reaction with O_2. Control experiments are conducted in the absence of NO to confirm that an immeasurable extent of oxidation has proceeded prior to NO addition.

[13] Experiments were conducted at room temperature (297 ± 3 K) at 445 and 750 torr pressure. The reaction time

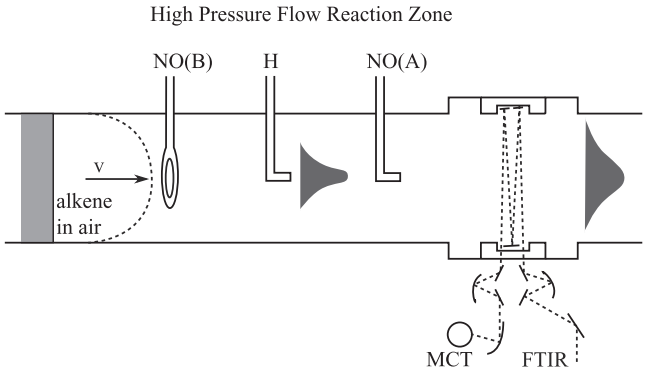

Figure 2. High-pressure flow system reaction zone. The flow tube is 6.3 cm in radius, and the total reaction length is ~70 cm. Reagent alkene is well mixed in air carrier gas 8 m upstream. H atoms are generated in a microwave discharge sidearm and enter at the center of the flow in argon carrier gas that comprises ~10% of the bulk flow. During product studies, 5% NO/N_2 is injected 8 cm farther downstream at position NO(A). OH is generated by the $H + O_2 \rightarrow HO_2$ and $HO_2 + NO \rightarrow OH + NO_2$ reactions. Products and residual reactants are measured 30 cm downstream at a 32-pass 15-cm base path White cell using a Mattson RS1 Fourier transfer infrared (FTIR) spectrometer with 1 cm^{-1} resolution. The White cell is oriented across the flow tube for high time resolution and samples a radially integrated average of concentration gradients. During NO sensitivity tests, ~0.04% NO in air is injected 38 cm upstream of the H atoms through a 3-cm radius annular injector at position NO(B). All HO_x has been removed prior to reaching the White cell.

from NO addition varied between experiments from 3.5 to 5.8 s with a mean velocity of 9.0 to 5.3 cm s^{-1}. H atom injection took place 8 cm upstream of NO addition. Carrier gas mixing ratios were 0.72 N_2, 0.18 O_2, and 0.10 Ar. Initial concentrations of alkene were near 10^{15} cm^{-3} and of NO were a few 10^{14} cm^{-3}. We cannot directly measure initial H or HO_2 concentrations, but based on experience with this radical source, they are a few 10^{12} cm^{-3} [*Dransfield et al.*, 2001]. See Table 1 for actual concentrations in each experiment. The timescale for oxidation at these reagent concentrations is only a few milliseconds. With diffusion coefficients of about 0.2 cm^2 s^{-1} at 750 torr, oxidation is expected to occur prior to full mixing of radical plumes into the bulk laminar carrier flow. Reported concentrations are radial averages and actual concentrations at the site of oxidation, as the radical plume mixes with alkene-containing carrier gas, can be as much as a factor of 10 lower. This conservative upper limit in the concentration gradient assumes mixing by diffusion alone, ignoring bulk mixing at the injector. Previously reported studies using reaction modulation spectroscopy [*Donahue et al.*, 1996a; *Clarke et al.*, 1998] were conducted at significantly lower pressures (9 torr) such that diffusion of the radical plume was rapid relative to the OH reaction time. Concentration gradient effects are examined during an NO sensitivity experiment discussed below.

[14] The OH + alkene reaction of interest was modulated via the H atom source every few minutes, with an H_2 flow on-off cycle, and changes in the infrared spectrum were monitored. Background (reactant only) spectra were collected with H_2 flow off and sample (product and residual reactant) spectra were collected with flow on. Infrared spectra were collected by a RS1 Mattson spectrometer using an axial 32-pass White cell with a 5-m total path length and <0.5-s time resolution. Typically, 300 scans are coadded at 1 cm^{-1} resolution, and six such spectra are averaged for a total of 12 min of sampling time.

[15] Reagent concentrations were carefully chosen to direct alkene oxidation toward the desired mechanistic pathway and eliminate secondary chemistry. Exploiting the differences in reactivity between $RO_2 + HO_2/RO_2$

Table 1. Initial and Product Concentrations (10^{13} cm^{-3})[a,b]

	Isoprene		Butadiene	
	750-torr Pressure	445-torr Pressure	750-torr Pressure	445-torr Pressure
Reaction time, s	5.8	4.9	5.8	3.5
Initial Alkene	145 (14)	290 (29)	142 (14)	294 (29)
Initial NO	80 (11)	100 (14)	78 (11)	50 (7)
Initial NO_2	5.0 (0.2)	0.50 (0.02)	5.0 (0.2)	0.260 (0.013)
Reacted Alkene	1.70 (0.17)	3.7 (0.4)	1.84 (0.18)	2.83 (0.28)
Reacted NO	3.8 (0.5)	6.0 (0.8)	4.1 (0.6)	6.61 (0.93)
Product NO_2	3.31 (0.17)	5.8 (0.3)	3.56 (0.18)	6.03 (0.30)
Acrolein			1.00 (0.07)	1.95 (0.14)
Furan			0.029 (0.007)	0.054 (0.004)
MVK	0.75 (0.07)	1.64 (0.16)		
MACR	0.48 (0.05)	1.00 (0.10)		
3MF	<0.03	<0.05		
CH_2O	1.13 (0.17)	2.2 (0.3)	1.06 (0.16)	1.96 (0.29)
CO	<0.02	<0.04	0.058 (0.006)	0.110 (0.011)
$HONO_2$	<0.05	<0.05	<0.02	<0.02
HONO	<0.3	0.5 (0.25)	<0.2	<0.2
$RONO_2$[c] at 835 cm^{-1}	0.15 (0.07)	0.24 (0.11)	0.13 (0.06)	0.19 (0.09)
$RONO_2$ at 1290 cm^{-1}	0.22 (0.10)	0.30 (0.14)	0.26 (0.12)	0.35 (0.17)
$RONO_2$ at 1660 cm^{-1}	0.22 (0.10)	0.38 (0.18)	0.21 (0.10)	0.39 (0.19)

[a]Upper limits are provided when species were not detected.
[b]Values in parentheses are 2-sigma uncertainties.
[c]Alkyl nitrate is measured as isopropyl nitrate. See text for details.

versus RO_2 + NO, we used elevated NO levels to assure that all RO_2 reaction proceeded with NO. Excess alkene ensures that secondary chemistry will remain insignificant, and an upper limit to secondary reaction can be established by using the measurement of CO, a dominant secondary product. Less than 1.5% of total alkene has reacted by experiment's end.

[16] In order to assess potential interferences from reagent axial concentration gradients or from competing chemistry such as RO + NO/NO_2 or RO_2 + HO_2/RO_2, we conducted two experiments probing different aspects of the experimental design. First, an NO sensitivity experiment was conducted for isoprene oxidation at 445 torr, in which the NO concentration was varied over a factor of 10, roughly 3 times below and above the concentration used in product studies. The NO was also injected in a different location and manner, 3.5 s prior to the H radical injection point (38 cm) through a 1/8″ OD 19-cm annular Teflon tube with 9 equidistant 0.020″ OD holes to accelerate mixing. Additionally, 10% of the air carrier flow was premixed within the NO line. This configuration doubles the NO_2 production from NO reaction with O_2. Second, all reagents other than H were mixed to test for NO_x reactions with the alkenes. Results from each test were compared with those for the configuration used in all other experiments. Product yields did not change over the tenfold variation in NO or from the changed configuration for NO introduction. At the lowest NO concentration a trace amount of $ROONO_2$ was detected. At the highest NO concentration, HONO was present at a few percent of reacted alkene levels. Changing the NO injection method also did not change the product distribution in the butadiene system. Finally, neither isoprene nor butadiene showed any measurable reaction with only NO_x present.

[17] The optical path length of the White cell was measured using dichlorodifluoromethane's IR cross section reported in the Hitran database (uncertainty <2% [*Rothman et al.*, 1998]) together with a separate in situ UV absorption concentration measurement at 185 nm. Reference IR spectra were collected within the high-pressure flow system [*Donahue et al.*, 1996b]. Reagents and standards were purchased from Aldrich Chemical Company, unless otherwise specified, and had the following purities: isoprene, 99%; butadiene, 99%; methyl vinyl ketone, 99%; methacrolein, 95%; acrolein, 97% (Acros Organics); 3-methyl furan, 98% (TCI America); furan, 99%; NO, 99% (Matheson Gases); NO_2, 99.5% (Matheson Gases); isopropyl nitrate, 99%; butadiene monoxide, 98%; butadiene diepoxide, 97%; and hydroxyacetone, 90%. CO reference spectra were generated from the line spectrum in the Hitran database [*Rothman et al.*, 1998] adjusting for pressure broadening and reduced spectral resolution (1 cm^{-1}) [*Donahue et al.*, 1996b]. The formaldehyde (VICI Metronics Incorporated high-emission permeation device) reference cross sections at 445 and 750 torr were calibrated at 0.01 cm^{-1} resolution on a Bruker IFS 120 high-resolution spectrometer using individual spectral lines in the Hitran database (5% or better accuracy [*Rothman et al.*, 1998]). A reference spectrum for *cis*- and *trans*-HONO was collected by reaction of OH + NO for which *cis* and *trans* isomer formation was assumed to be equal, and the integrated cross section for *trans*-HONO near 1255 cm^{-1} was assigned on the basis of the work of *Becker et al.* [1995]. The alkene spectra remained linear at the highest experimental concentrations, but NO's spectrum was highly nonlinear. Pseudo cross sections for NO at 445 and 750 torr were created from difference spectra generated with small, known concentration changes ($\sim 4 \times 10^{13}$ cm^{-3}) above substantial background concentrations (8×10^{14} cm^{-3}). The error in measured Δ[NO] using Beer's law and the pseudo cross sections was determined by analyses of known concentrations in the range $(1-10) \times 10^{13}$ cm^{-3} above a background concentration of (4 or 8) $\times 10^{14}$ cm^{-3}.

3. Results

[18] Resulting spectra are shown in Figure 3. The red line is raw data, showing the depletion of reactants alkene and NO (negative absorbance) as well as the product formation (positive absorbance). The residual spectrum (black solid line) indicates that additional species are produced, most notably in alkyl nitrate (835, 1290, 1660 cm^{-1}), hydroxyl (1050 cm^{-1}) and carbonyl (1700 cm^{-1}) regions of the spectrum. The noise level in these spectra is approximately 50 ppm fractional absorption, or 175 ppm $min^{1/2}$.

[19] Alkyl nitrate bands were measured as isopropyl nitrate, with integrated cross sections assigned as follows (±10%, base e, cm $molecule^{-1}$): 835 $cm^{-1} = 2.8 \times 10^{-17}$, 1290 $cm^{-1} = 2.4 \times 10^{-17}$, 1660 $cm^{-1} = 4.9 \times 10^{-17}$. Density functional theory (DFT) calculations were used to assess the suitability of using isopropyl nitrate cross sections for butadiene and isoprene hydroxy alkyl nitrates. DFT B3LYP calculations (6–31g(d,p) basis) for nitric acid and isopropyl nitrate were compared with actual integrated band intensities for the three major nitrate features in this region: NO stretch near 835 cm^{-1}, the mixed feature near 1290, and NO_2 asymmetric stretch at 1660. Theoretical calculations were consistent with actual cross sections to within 8% (2 sigma), supporting the use of DFT for this comparison. Theoretical calculations were performed for the four hydroxy nitrate isomers formed from butadiene. The band cross sections had the following average ratios to isopropyl nitrate bands with the corresponding variability (2 sigma): 1.13 ± 50% (835 cm^{-1}), 1.05 ± 12% (1290 cm^{-1}) and 0.99 ± 10% (1660 cm^{-1}). The first band near 835 cm^{-1} is the most variable, and the other two bands have a very small change in total cross section. On the basis of these results, isopropyl nitrate cross sections were used without further adjustment.

[20] Specific identification of the peroxynitrate isomers produced in these systems is not possible in the midinfrared. However, because the band locations, shapes, and intensities are so similar for these species, we can usefully constrain the average cross section and thus determine the integrated nitrate yield. To accomplish this, butadiene (1.5 ± 10^{14} molecules cm^{-3}) was reacted with OH in air in the presence of NO_2 (3.2×10^{14} molecules cm^{-3}) at 50 torr to obtain a spectrum of peroxynitrate (see Figure 4). By equating reacted [butadiene] to total [peroxynitrate], the three major peroxynitrate features were assigned the following average integrated cross sections (±25%, base e, cm $molecule^{-1}$): 792 $cm^{-1} = 1.03 \times 10^{-17}$; 1297 $cm^{-1} = 2.36 \times 10^{-17}$; 1720 $cm^{-1} = 3.06 \times 10^{-17}$. The integrated cross section for the 1297 cm^{-1} band agrees well with previous peroxynitrate measurements (c-$C_6H_{11}OONO_2$,

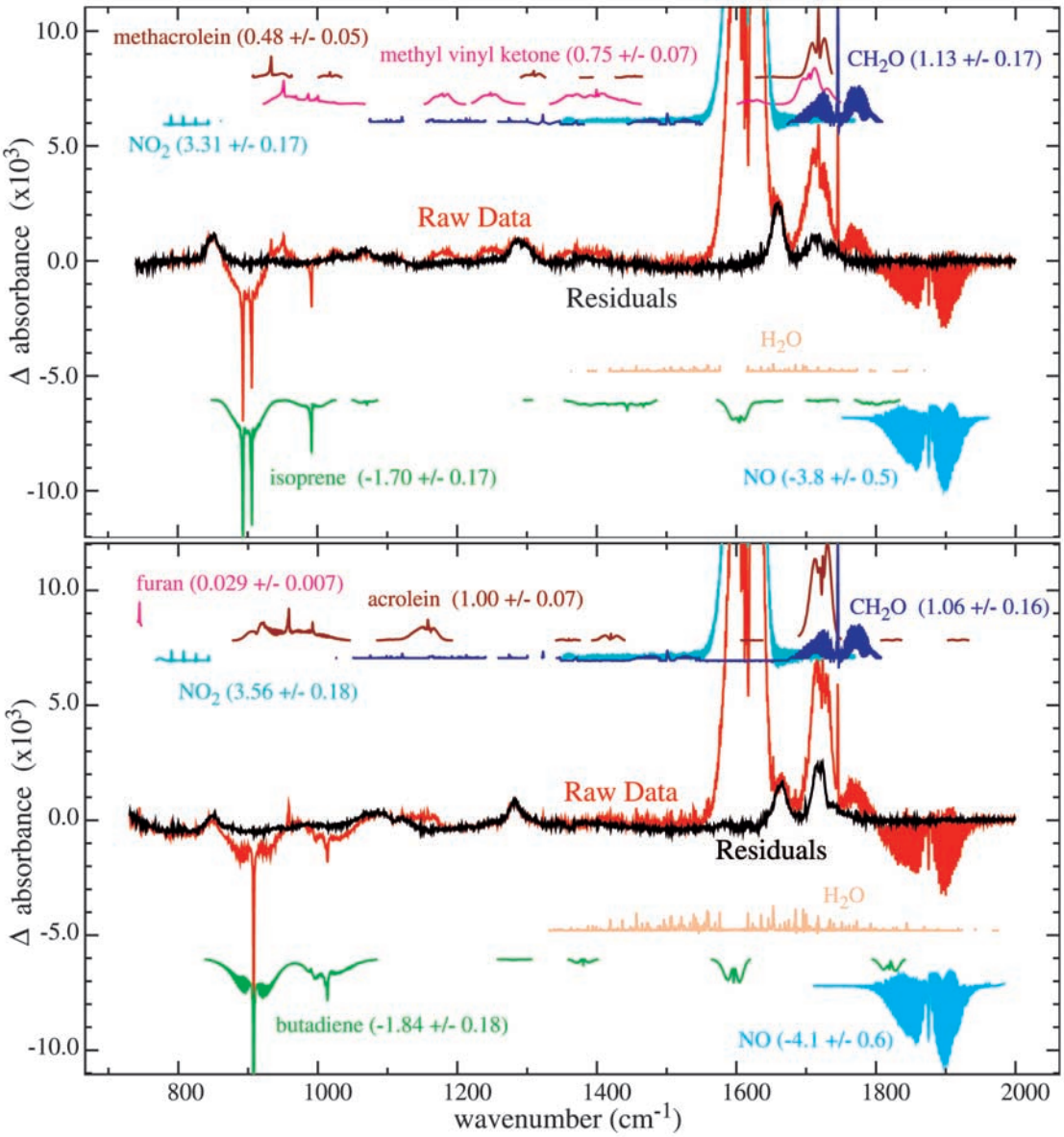

Figure 3. (top) Isoprene and (bottom) butadiene reaction spectra and residuals at 750 torr. Concentrations are reported in $\times 10^{13}$ cm^{-3}. The abscissa is the change in absorbance (ln) between spectra taken with the H_2 flow on and off. Reactants have negative absorbance, and products have positive absorbance. The raw spectrum is shown in red. Product and reactant reference spectra are color coded and scaled to the concentrations used for spectral subtraction. The residual spectrum is shown by the black solid line; and for both isoprene and butadiene, oxidation shows additional products in the alkyl nitrate (835, 1290, 1660 cm^{-1}), hydroxyl (1050 cm^{-1}) and carbonyl (1700 cm^{-1}) regions.

2.48×10^{-17} [*Platz et al.*, 1999]; $CH_3C(O)O_2NO_2$, 2.58×10^{-17} [*Tuazon and Atkinson*, 1990a]).

[21] The spectral analyses are summarized in Table 1. Reacted alkene and dominant unsaturated carbonyl products, methyl vinyl ketone, methacrolein, and acrolein, are reported to within 10% accuracy (2 sigma). Aggregate alkyl nitrate yields are based upon cross sections for isopropyl nitrate and are reported separately for each of the three major nitrate bands. Bands at 1290 and 1660 cm^{-1} agree well, with the band at 835 consistently giving a lower yield. As previously discussed, the 835 cm^{-1} band is the least reliable because of likely changes in cross section between isopropyl nitrate and the isoprene hydroxy nitrates. CO, $HONO_2$, and $ROONO_2$ were analyzed to verify that secondary or interfering chemistry was insignificant. Nitric acid was never detected. Carbon monoxide was not detected during isoprene oxidation experiments but was measured as a 3% yield in the oxidation of butadiene. Trace $ROONO_2$ was detected in only a single experiment, butadiene oxidation at 445 torr. HONO was barely detectable in all but one of the experiments, isoprene oxidation at 445 torr, where it was ~13% of reacted alkene. Some

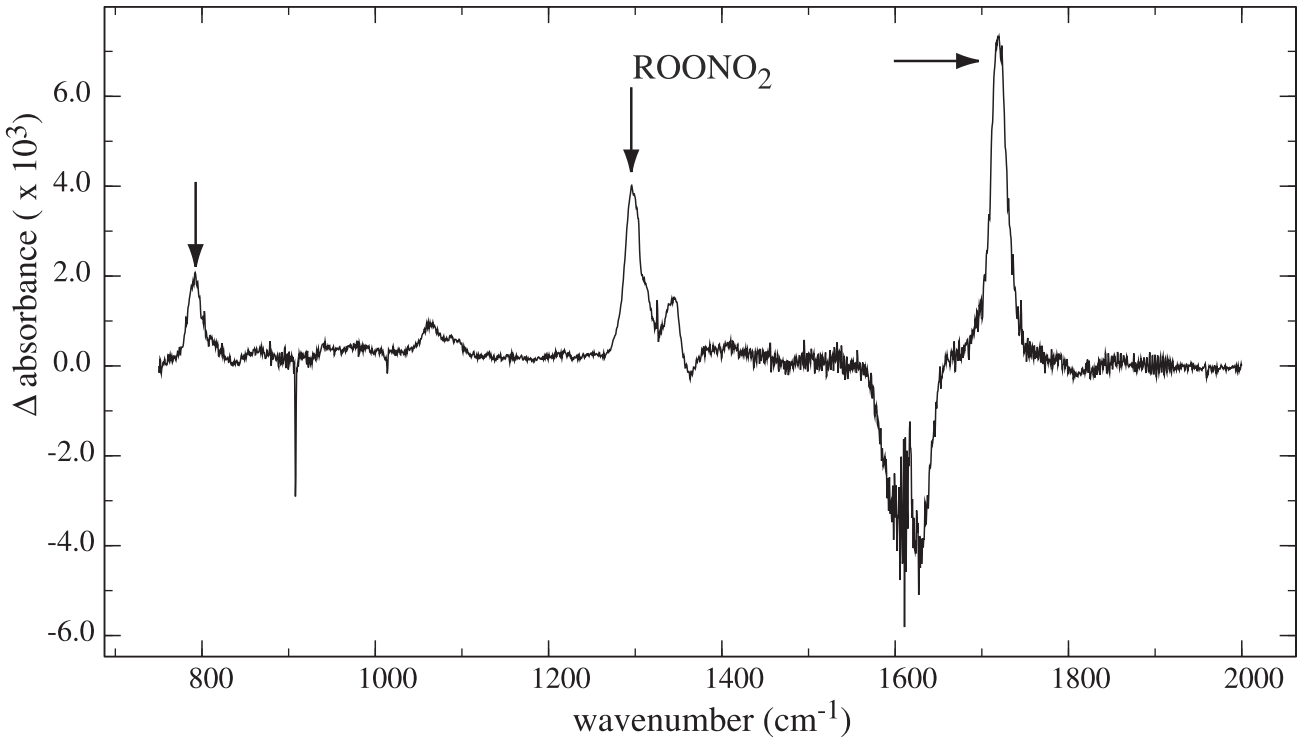

Figure 4. $ROONO_2$ from butadiene. Three major bands are indicated by arrows. $HONO_2$ and mirror contaminant are present at ~1300–1360 cm^{-1}, and OH bands are present from 1050 to 1100 cm^{-1}; butadiene, NO_2, and NO are also present (see Figure 3 for their reference spectra).

HONO is expected from the OH + NO reaction, and its presence does not interfere with the isoprene oxidation study.

[22] In Table 2 the results at 750 and 445 torr are reported as fractional yields and are compared with previous studies of these reactions conducted at or near 750 torr. The carbonyl measurements for isoprene oxidation are slightly higher than previous studies but are consistent within experimental uncertainties. Carbonyl species for butadiene agree very well with the recent study of *Tuazon et al.* [1999]. The results for the furans differ from previous studies: 3-methyl furan is not detected during isoprene's oxidation, and furan's yield from butadiene (1.6%) is less than half of the recent *Tuazon et al.* [1999] result. At 750 torr, alkyl nitrate yields of 12% and 11% are found for isoprene and butadiene, respectively. These levels are higher

Table 2. Fractional Yields Compared With Previous Studies[a,b]

	Isoprene					
	Tuazon and Atkinson [1990a]	*Paulson et al.* [1992]	*Miyoshi et al.* [1994]	*Chen et al.* [1998]	Present Work	
					750 torr	445 torr
MVK	0.32 (0.07)	0.36 (0.04)	0.32 (0.05)		0.44	0.44 (0.06)
MACR	0.22 (0.05)	0.25 (0.03)	0.22 (0.02)		0.28	0.27 (0.04)
MVK+MACR	0.54 (0.09)	0.61 (0.05)	0.54 (0.05)		0.72	0.71 (0.07)
MVK/MACR	1.4 (0.5)	1.4 (0.2)	1.45 (0.18)		1.6	1.6 (0.2)
CH_2O	0.63 (0.10)		0.57 (0.06)		0.66	0.59 (0.12)
3MF	0.048 (0.006)	0.04 (0.02)			<0.02	<0.01
$RONO_2$	0.08–0.14			0.044 (0.008)	0.12	0.08 (0.06)
Carbonyls	0.21–0.27					
	Butadiene					
	Tuazon et al. [1999]	*Maldotti et al.* [1980]	*Ohta* [1984]	*Atkinson et al.* [1989]	Present Work	
					750 torr	445 torr
Acrolein	0.58 (0.04)	0.98 (0.12)	0.39		0.54	0.69 (0.07)
CH_2O	0.62 (0.05)				0.58	0.69 (0.10)
Furan	0.035 (0.005)		0.06 (0.02)	0.039 (0.011)	0.016	0.019 (0.002)
$RONO_2$	0.07 (0.03)				0.11	0.11 (0.06)

[a]Upper limits are provided when species were not detected.
[b]Values in parentheses are 2-sigma uncertainties.

than previous findings, nearly 3 times greater than the isoprene results of *Chen et al.* [1998] but identical with the isoprene results of *Tuazon and Atkinson* [1990a] and 60% higher than the butadiene results of *Tuazon et al.* [1999], which remains within experimental error. (Note that in the work of *Tuazon and Atkinson* [1990a] and *Tuazon et al.* [1999], alkyl nitrate was analyzed at a single band, 1290 cm^{-1}, with an assigned cross section 15% and 25% higher, respectively, than our estimate.)

[23] Additional species detected in previous product studies [*Liu et al.*, 1999] or known as subsequent oxidation products [*Atkinson*, 1997a], hydroxyacetone, butadienemonoxide, butadienediepoxide, and glycolaldehyde, were not detected in our experiments. We conclude that these species are not significant (greater than a few percent yield) first-stage products in the oxidation of butadiene or isoprene.

4. Discussion

4.1. Oxidation Mechanism and Competing Chemistry

[24] The fractional product yields in Table 2 are assumed to result from the following reaction sequence illustrated in Figure 5 for butadiene: (1) OH addition to alkene, (2) O_2 addition to the resulting hydroxyalkyl radical, (3) NO reaction with the product hydroxyalkylperoxy radical which forms either (3a) an unsaturated hydroxyalkoxy radical and NO_2 or (3b) alkyl nitrate, and, finally, (4) C-C bond fission and H atom abstraction by O_2 to form a stable unsaturated carbonyl, HO_2, and formaldehyde. The OH-alkene adduct has resonance forms that produce alkoxy radicals incapable of C-C bond fission at step 4. These isomers undergo H abstraction by O_2 or 1,5 H shift isomerization at step 4 and are thought to produce mostly unsaturated hydroxycarbonyls not measurable in the present experiment. See Figure 1 for more details about isoprene oxidation and reactions of the resonance forms of the OH-alkene adduct. The mechanism for furan ring formation is not fully understood and is discussed in section 4.3. Potential competitive reaction pathways under experimental conditions must be considered at each of the four reaction steps and ruled insignificant prior to assigning the fractional yields solely to this mechanism.

[25] The initial reaction (step 1) of alkene with OH occurs primarily via addition, and any H abstraction has been neglected. Recent work of *Campuzano-Jost et al.* [2000] puts the isoprene abstraction pathway at less than 5% of overall reaction; on the basis of typical abstraction rates it is probably less than 1%. Rate constants at room temperature and pressure for the reactions with OH are $(1.0 \pm 0.1) \times 10^{-10}$ cm^3 s^{-1} for isoprene [*Campuzano-Jost et al.*, 2000; *Chuong and Stevens*, 2000; *Zhang et al.*, 2000] and $(6.7 \pm 0.2) \times 10^{-11}$ cm^3 s^{-1} for 1,3-butadiene [*Atkinson and Aschmann*, 1984]. Control experiments were conducted to confirm that H atom and NO_2 reactions with alkene were not important competitive reactions (see section 2 [see also *Chuong and Stevens*, 2000; *Clarke et al.*, 2000; *Paulson et al.*, 1992]).

[26] Formation of peroxy radicals in step 2 has no probable competitors because of the high levels of O_2 present. The recently measured (R. Zhang, unpublished results, 2001) rate constant for this reaction in the isoprene system of $(7 \pm 3) \times 10^{-13}$ cm^3 s^{-1} is consistent with previously reported measurements of alkyl + O_2 reaction rates. At this rate of reaction, there are no significant competitive channels.

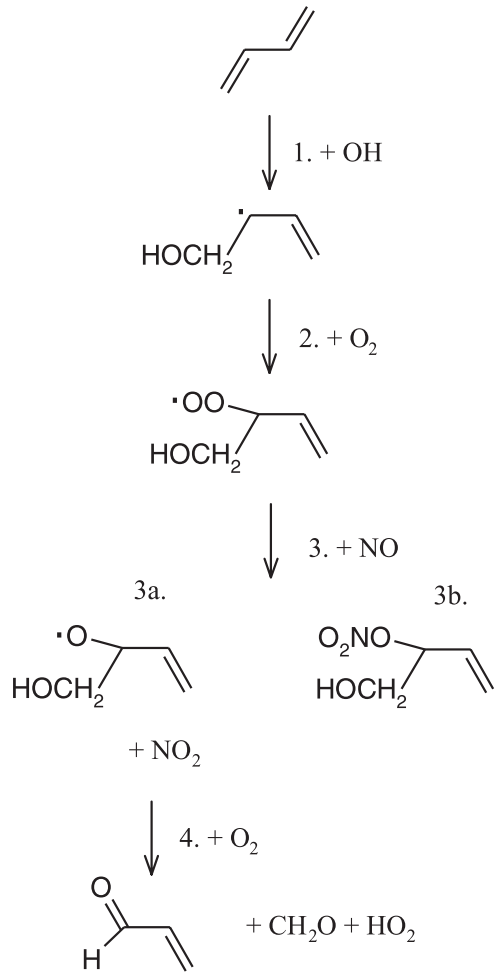

Figure 5. Generic oxidation scheme shown for OH addition to end carbon of butadiene. Resonance of free radical following first reaction step is excluded. Resonance forms undergo H abstraction by O_2 or 1,5 H shift isomerization at step 4. See Figure 1 for more details about isoprene oxidation and step 4.

[27] The next reaction (step 3) of the unsaturated hydroxyperoxy radical with NO has several competitors: NO_2, HO_2, and self reactions. Reaction with NO_2 occurs at a similar rate to NO; thus with NO_2 present at several percent of NO levels, this reaction is likewise expected to occur at several percent of the NO reaction. However, the product $ROONO_2$ has a lifetime of about 1 s [*Kirchner et al.*, 1999] and will dissociate. Its final concentration 3–6 s later at the IR detection region is significantly smaller, less than 1% of reacted alkene. As expected, the highest levels (a few percent) of $ROONO_2$ were observed during the NO sensitivity experiment under conditions of lowered NO and elevated NO_2. While the $ROONO_2$ yield is very small, one of its bands overlaps with $RONO_2$ in the 1290 cm^{-1} region of the IR spectrum. For this reason its absence from product studies was confirmed in two ways: by the absence

of any spectral features near its band at 792 cm^{-1} and also by measuring three separate $RONO_2$ spectral bands at 835, 1290, and 1660 cm^{-1}. Results for each of these three bands is reported independently in Table 1. The variability in results for the three bands most likely reflects inaccuracies in using isopropyl nitrate as a calibration reference, and the band at 1290 cm^{-1} shows no evidence of cross contamination from $ROONO_2$.

[28] Potential interference from $RO_2 + HO_2/RO_2$ to reaction 3 was assessed in two ways: by varying the experimental conditions and by modeling the competitive chemistry. We shall address these in turn. Direct detection of the unique carbonyl and alcohol products from these reactions is difficult, as they have no strong spectroscopic features that distinguish them from similar products of the NO reaction channel. However, if these reactions had been significant competitors during the product studies, then large changes in measured product yields should have been observed during the NO sensitivity experiments, in which the average concentration of NO was varied by a factor of 10, and the point of injection for NO was placed before the H atom source and compared with results when NO was injected downstream of the H atom source. As reported in section 2, only changes in HONO and $ROONO_2$ were observed, indicating that $RO_2 + HO_2/RO_2$ chemistry cannot account for more than a few percent of total reaction under the conditions of our study.

[29] To calculate the potential significance of $RO_2 + HO_2/RO_2$ chemistry, we used a simple chemical model [*Donahue and Prinn*, 1990] in which the RO_2 rates of reaction were (in $cm^3\ s^{-1}$) the following: NO, 9.0×10^{-12} [*Eberhard and Howard*, 1997; *Stevens et al.*, 1999]; RO_2, 5.8×10^{-12} [*Jenkin et al.*, 1998]; and HO_2, 1.6×10^{-11} [*Jenkin et al.*, 1997]. The RO_2 and HO_2 rates have not been measured directly, and conservative upper limits were used to maximize the competitive channels. All rate uncertainties exceed a factor of 2. By using average isoprene experimental conditions at 750 torr, total products from $RO_2 + RO_2$ and $RO_2 + HO_2$ channels were less than 0.2%. The extent of competitive chemistry was most sensitive to NO levels, which were likely lower in the radical plume at the time of oxidation because of incomplete mixing. The reduction of [NO] in the model by a factor of 10 resulted in greater HO_2/RO_2 competitive chemistry, still less than a few percent of total reaction.

[30] Finally, the fate of the unsaturated hydroxyalkoxy radical produced in step 3a must be considered. Rapid C-C bond fission (step 4) leads to the measured products of acrolein, MVK, and MACR. Other alkoxy radicals undergo either 1,5 H shift isomerization or slower H atom abstraction by O_2 (see Figure 1 for examples). The major competitive channels are alkoxy combination with NO or NO_2 to form RONO and $RONO_2$, respectively. Rates of reaction for these processes are not known. However, on the basis of measured rates for analogous reactions [*DeMore et al.*, 1997; *Atkinson*, 1997b], NO and NO_2 interference could only be significant to <10% percent and only for alkoxy radicals undergoing slow 1,5 H shifts or H atom abstraction. IR spectroscopy can be used to confirm the absence of significant RONO in product studies (detection limit is <4% yield [*Niki and Maker*, 1990]), with *cis* and *trans* isomeric features present from 770 to 820 cm^{-1}. The competitive reaction of $RO + NO_2$ to form $RONO_2$ would interfere with an assessment of the atmospherically important reaction of $RO_2 + NO$ to form $RONO_2$. However, we use RONO as an indirect tracer of this process. Under our experimental conditions, NO levels always exceeded NO_2 levels, and thus RONO formation would always exceed $RONO_2$ formation from RO. We did not observe any RONO, indicating that the measured $RONO_2$ is formed exclusively from the reaction of $RO_2 + NO$. In addition, $RONO_2$ yields were invariant under large changes in [NO] and [NO_2] during the NO sensitivity experiment, demonstrating that these competitive channels are not significant.

4.2. Secondary Chemistry

[31] The presence of a 3% yield of CO in the oxidation of butadiene is most likely due to secondary chemistry enabled by a concentration gradient. Because of its low detection threshold and its formation in the OH oxidation of carbonyl species such as the primary products CH_2O, acrolein, and methacrolein, CO production can be used to set an upper limit on the extent of secondary chemistry during the oxidation experiments. We doubt that CO is a first-stage oxidation product. DFT B3LYP energy calculations (6–31g(d,p) basis) for peroxy internal attack of the C = C bond, the most energetically favored mechanism for prompt CO formation [*Demerjian et al.*, 1974], indicate that the reaction is endothermic by a few kilocalories and presumably not important. CO is formed in the secondary oxidation of CH_2O and acrolein by OH, with rates of reaction of 1.0×10^{-11} $cm^3\ s^{-1}$ [*DeMore et al.*, 1997] and 1.8×10^{-11} $cm^3\ s^{-1}$ [*Atkinson et al.*, 1983], respectively. The CO yield in acrolein oxidation is not well understood, but comparison with methacrolein oxidation [*Tuazon and Atkinson*, 1990b] indicates that up to 40% of reacted acrolein forms CO after addition of OH at the C3 position, which in the presence of high NO ultimately forms glycolaldehyde and HCO. HCO rapidly reacts with O_2 to form HO_2 and CO.

[32] Butadiene's rate of reaction with OH is thus 4 times faster than the total CO forming rate (k_{OH} for butadiene versus k_{OH} for $CH_2O + 0.4 \times k_{OH}$ for acrolein) [*Atkinson*, 1997a], indicating that 12% of butadiene must react for a corresponding CO yield of 3%, as measured in the butadiene product study at 750 torr. This result assumes that CO is not formed by the oxidation of other primary carbonyl products, such as the hydroxycarbonyl species. Although only 1.3% of butadiene reacts during the oxidation experiments, a concentration gradient could allow for a localized, greater depletion of butadiene. Measured concentrations are integrated radially across the reaction flow tube, and the radical plume will not be fully mixed with the bulk flow prior to its reaction. A total CO yield of 3% therefore constrains the total secondary chemistry during the oxidation of butadiene to less than 10%. Another product of acrolein oxidation, glycolaldehyde, was not observed, but it has a higher detection limit than CO.

[33] CO was not detected in isoprene oxidation experiments. Isoprene's rate of reaction with OH is 50% faster than butadiene's, and methyl vinyl ketone oxidation by OH does not immediately lead to CO [*Tuazon and Atkinson*, 1989]. Thus a significantly larger depletion of local isoprene would be required before measurable levels of CO could be formed by secondary chemistry. Secondary chemistry for

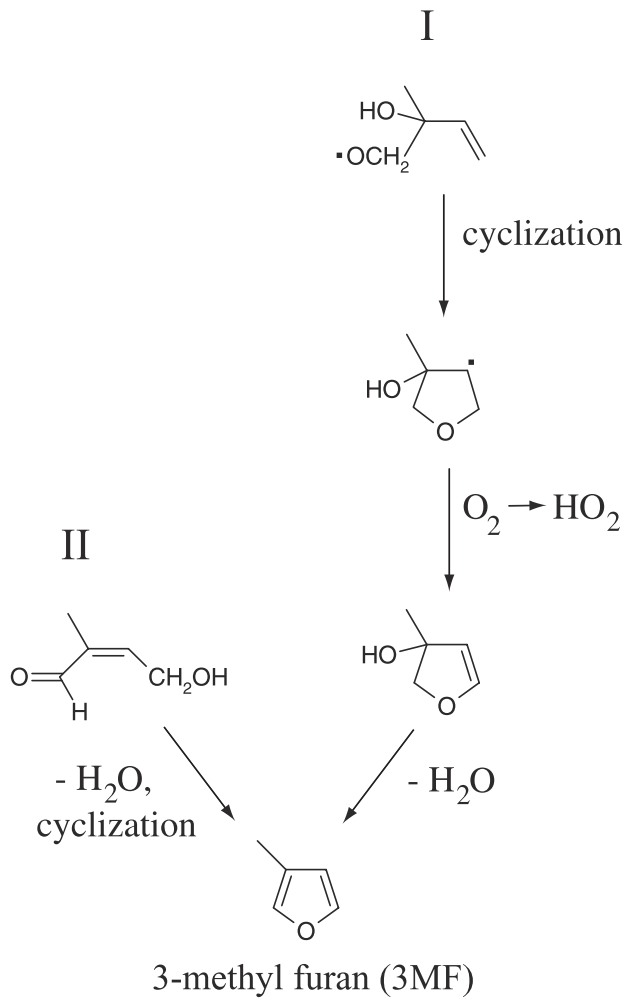

Figure 6. Possible mechanisms for 3-methyl furan formation [*Gu et al.*, 1985; *Tuazon and Atkinson*, 1990a].

isoprene was less than that for butadiene because of its faster rate of reaction with OH and otherwise similar experimental conditions.

4.3. Furan Ring Formation

[34] Two mechanisms have been proposed for furan ring formation by the oxidation of isoprene and are shown in Figure 6. The intermediate in the first mechanism, 2,3-dihydro-3-hydroxy-3-methylfuran, is known to be stable at room temperature (D. Hausmann, unpublished results, 2000), and so is unlikely to proceed to 3-methyl furan formation within the few seconds of the present product studies. In addition, C-C bond fission of the alkoxy radical in the first mechanism is thought to be extremely rapid with a rate around 10^{13} s^{-1}. This fact adds the unlikely requirement that cyclization be similarly fast to compete [*Dibble*, 1999]. The absence of 3-methyl furan in the present product study for isoprene cannot a posteriori eliminate either mechanism as a possibility. However, the observation of furan in the oxidation of butadiene indicates that it is a first-stage product formed within a few seconds. This evidence favors the second mechanism because of the stability of 2,3-dihydro-3-hydroxyfuran, an intermediate in the first mechanism for butadiene. Mechanism II relies on a ring closure that readily occurs in solution, but the present experiment with butadiene indicates its possibility in the gas phase as well.

4.4. Alkyl Nitrate Yields

[35] The alkyl nitrate yields in the present study are consistent with upper limits in previous studies but are nearly a factor of 3 greater than the more detailed study of *Chen et al.* [1998] (see Table 2). This difference in yield cannot be attributed to deviations in the alkyl nitrate cross sections from the isopropyl nitrate standard or to experimental uncertainty. The agreement between the two features at 1290 and 1660 cm^{-1} as well as the insensitivity of the alkyl nitrate yield to tenfold changes in NO concentrations support our findings. The most likely interferences from RO + NO_2 or $ROONO_2$ have also been eliminated by the absence of RONO or $ROONO_2$ in other regions of the spectrum. Also, $ROONO_2$ would not overlap the 1660 cm^{-1} feature, but would appear at 1720 cm^{-1}. In the experiment of *Chen et al.* [1998] samples were extracted and analyzed by gas chromatography (GC), a method that might favor systematically lowered alkyl nitrate yields. Their result also depends upon accurate measurement of a small percentage change in isoprene concentration using GC. Full assessment of the large difference in results would best be accomplished by simultaneous analysis that made use of both in situ FTIR and sample extraction with gas chromatography.

5. Conclusions

[36] The RMS experimental approach to elucidating oxidation yields for atmospherically important hydrocarbons eliminates wall interactions, minimizes secondary chemistry, and avoids the presence of $O(^3P)$ atoms and ozone found in smog chamber studies [*Paulson et al.*, 1992]. We have focused on three products of substantial importance to our current understanding of isoprene and butadiene oxidation mechanisms: unsaturated carbonyls, furans, and hydroxynitrates. Here we observed yields of unsaturated carbonyls consistent with previous experiments but with far less furan formation (none in the case of 3MF from isoprene). The total ring formation observed in environmental chambers may require heterogeneous chemistry or longer reaction times. We observed alkyl nitrate yields consistent with the upper limits of previous studies but nearly a factor of 3 higher than a recent experiment [*Chen et al.*, 1998] that relied on sample extraction and subsequent GC analysis. This suggests that up to one fifth of total NO_x emissions can be removed by alkyl nitrate formation in regions with high isoprene emissions.

[37] The present product studies for isoprene and butadiene demonstrate that changes in reagent concentrations of just a few percent can be measured accurately by FTIR spectroscopy by modulation of a radical reagent. Molecular products were formed by as many as four reaction steps. As spectroscopic sensitivity improves, oxidation mechanisms may be examined in greater detail at each elementary step. The peroxynitrate spectrum shown in Figure 4 demonstrates one approach to arresting the oxidation process one step at a time: by complete conversion of the radicals to stable molecular species (with excess NO_2 in this case). If the

cross sections were known, the branching ratio for OH attack on butadiene could be determined by spectral features in the microwave or far-IR regions in which the peroxynitrate isomers are resolved.

[38] **Acknowledgments.** This work was supported by U.S. Environmental Protection Agency STAR grant (R825258010) to SUNY at Albany and Harvard University and National Science Foundation grant (9977992) to Harvard University. We are grateful to Timothy Dransfield and Jesse Kroll for helpful comments.

References

Abbatt, J. P. D., K. L. Demerjian, and J. G. Anderson, A new approach to free-radical kinetics: Radially and axially resolved high-pressure discharge flow with results for hydroxyl + (ethane, propane, n-butane, n-pentane) → products at 297 K, *J. Phys. Chem.*, *94*(11), 4566 –4575, 1990.

Atkinson, R., Gas-phase tropospheric chemistry of volatile organic compounds, 1, Alkanes and alkenes, *J. Phys. Chem. Ref. Data*, *26*(2), 215–290, 1997a.

Atkinson, R., Atmospheric reactions of alkoxy and β-hydroxyalkoxy radicals, *Int. J. Chem. Kinet.*, *29*(2), 99–111, 1997b.

Atkinson, R., and S. M. Aschmann, Rate constants for the reaction of OH radicals with a series of alkenes and dialkenes at 295 ± 1 K, *Int. J. Chem. Kinet.*, *16*, 1175–1186, 1984.

Atkinson, R., S. M. Aschmann, and J. N. Pitts Jr., Kinetics of the gas-phase reactions of hydroxyl radicals with a series of a α, β-unsaturated carbonyls at 299 ± 2 K, *Int. J. Chem. Kinet.*, *15*(1), 75–81, 1983.

Atkinson, R., S. M. Aschmann, E. C. Tuazon, J. Arey, and B. Zielinska, Formation of 3-methylfuran from the gas-phase reaction of OH radicals with isoprene and the rate constant for its reaction with the OH radical, *Int. J. Chem. Kinet.*, *21*(7), 593–604, 1989.

Becker, K. H., J. Kleffmann, R. Kurtenbach, P. Wiesen, A. Febo, M. Gherardi, and R. Sparapani, Line Strength measurements of trans-HONO near 1255 cm^{-1} by tunable diode laser spectrometry, *Geophys. Res. Lett.*, *22*(18), 2485–2488, 1995.

Biesenthal, T. A., Q. Wu, P. B. Shepson, H. A. Wiebe, K. G. Anlauf, and G. I. Mackay, A study of relationships between isoprene, its oxidation products, and ozone in the Lower Fraser Valley, BC, *Atmos. Environ.*, *31*(14), 2049–2058, 1997.

Campuzano-Jost, P., M. B. Williams, L. D'Ottone, and A. J. Hynes, Kinetics of the OH-initiated oxidation of isoprene, *Geophys. Res. Lett.*, *27*(5), 693–696, 2000.

Chen, X., D. Hulbert, and P. B. Shepson, Measurement of the organic nitrate yield from OH reaction with isoprene, *J. Geophys. Res.*, *103*, 25,563–25,568, 1998.

Chuong, B., and P. S. Stevens, Kinetic Study of the OH + isoprene and OH + ethylene reactions between 2 and 6 torr and over the temperature range 300–423 K, *J. Phys. Chem. A*, *104*, 5230–5237, 2000.

Clarke, J. S., J. H. Kroll, N. M. Donahue, and J. G. Anderson, Testing frontier orbital control: Kinetics of OH with ethane, propane, and cyclopropane from 180 to 360 K, *J. Phys. Chem. A*, *102*(48), 9847–9857, 1998.

Clarke, J. S., H. A. Rypkema, J. H. Kroll, N. M. Donahue, and J. G. Anderson, Multiple excited states in a two-state crossing model: Predicting barrier height evolution for H + alkene addition reactions, *J. Phys. Chem. A.*, *104*, 4458–4468, 2000.

Demerjian, K. L., J. A. Kerr, and J. G. Calvert, The mechanism of photochemical smog formation, *Adv. Environ. Sci. Technol*, *4*, 1–262, 1974.

DeMore, W. B., S. P. Sander, D. M. Golden, R. F. Hampson, M. J. Kurylo, C. J. Howard, A. R. Ravishankara, C. E. Kolb, and M. J. Molina, Chemical kinetics and photochemical data for use in stratospheric modeling, *JPL Publ.*, *97-4*, 1997.

Dibble, T. S., A Quantum chemical study of the C-C bond fission pathways of alkoxy radicals formed following OH addition to isoprene, *J. Phys. Chem. A*, *103*, 8559–8565, 1999.

Donahue, N. M., and R. G. Prinn, Nonmethane hydrocarbon chemistry in the remote marine boundary, *J. Geophys. Res.*, *95*, 18,387–18,411, 1990.

Donahue, N. M., K. L. Demerjian, and J. G. Anderson, Reaction modulation spectroscopy: A new approach to quantifying reaction mechanisms, *J. Phys. Chem.*, *100*(45), 17,855–17,861, 1996a.

Donahue, N. M., J. S. Clarke, K. L. Demerjian, and J. G. Anderson, Free-radical kinetics at high pressure: A mathematical analysis of the flow reactor, *J. Phys. Chem.*, *100*(14), 5821–5838, 1996b.

Dransfield, T. J., N. M. Donahue, and J. G. Anderson, High-pressure flow reactor product study of the reactions of $HO_x + NO_2$: The role of vibrationally excited intermediates, *J. Phys. Chem. A*, *105*(9), 1507–1514, 2001.

Eberhard, J., and C. J. Howard, Rate coefficients for the reactions of some C3 to C5 hydrocarbon peroxy radicals with NO, *J. Phys. Chem. A*, *101*, 3360–3366, 1997.

Goldan, P. D., D. D. Parrish, W. C. Kuster, M. Trainer, S. A. McKeen, J. Holloway, B. T. Jobson, D. T. Sueper, and F. C. Fehsenfeld, Airborne measurements of isoprene, CO, and anthropogenic hydrocarbons and their implications, *J. Geophys. Res.*, *105*, 9091–9105, 2000.

Grosjean, D., E. L. Williams II, and E. Grosjean, Atmospheric chemistry of isoprene and of its carbonyl products, *Environ. Sci. Technol.*, *27*, 830–840, 1993.

Gu, C.-L., C. M. Rynard, D. G. Hendry, and T. Mill, Hydroxyl radical oxidation of isoprene, *Environ. Sci. Technol.*, *19*, 151–155, 1985.

Guenther, A., et al., A global model of natural organic compound emissions, *J. Geophys. Res.*, *100*, 8873–8892, 1995.

Jenkin, M. E., and G. D. Hayman, Kinetics of reactions of primary, secondary and tertiary b-hydroxy peroxyl radicals, *J. Chem. Soc. Faraday Trans.*, *91*(13), 1911–1922, 1995.

Jenkin, M. E., S. M. Saunders, and M. J. Pilling, The tropospheric degradation of volatile organic compounds: A protocol for mechanism development, *Atmos. Environ.*, *31*, 81–104, 1997.

Jenkin, M. E., A. A. Boyd, and R. Lesclaux, Peroxy radical kinetics resulting from the OH–initiated oxidation of 1,3-butadiene, 2,3-dimethyl-1,3-butadiene and isoprene, *J. Atmos. Chem.*, *29*, 267–298, 1998.

Killus, J. P., and G. Z. Whitten, Isoprene: A photochemical kinetic mechanism, *Environ. Sci. Technol.*, *18*(3), 142–148, 1984.

Kirchner, F., A. Mayer-Figge, F. Zabel, and K. H. Becker, Thermal stability of peroxynitrates, *Int. J. Chem. Kinet.*, *31*(2), 127–144, 1999.

Kwok, E. S. C., R. Atkinson, and J. Arey, Observation of hydroxycarbonyls from the OH radical-initiated reaction of isoprene, *Environ. Sci. Technol.*, *29*(9), 2467–2469, 1995.

Lei, W., A. Derecskei-Kovacs, and R. Zhang, *Ab initio* study of OH addition reaction to isoprene, *J. Chem. Phys.*, *113*(13), 5354–5360, 2000.

Lei, W., R. Zhang, W. S. McGivern, A. Derecskei-Kovacs, and S. W. North, Theoretical study of OH-O_2-isoprene peroxy radicals, *J. Phys. Chem. A*, *105*, 471–477, 2001.

Liu, X., H. E. Jeffries, and K. G. Sexton, Hydroxyl radical and ozone initiated photochemical reactions of 1,3-butadiene, *Atmos. Environ.*, *33*(18), 3005–3022, 1999.

Maldotti, A., C. Chiorboli, C. A. Bignozzi, C. Bartocci, and V. Carassiti, Photooxidation of 1,3-butadiene containing systems: Rate constant determination for the reaction of acrolein with OH radicals, *Int. J. Chem. Kinet.*, *12*, 905–913, 1980.

McKeen, S. A., et al., Photochemical modeling of hydroxyl and its relationship to other species during the Tropospheric OH Photochemistry Experiment, *J. Geophys. Res.*, *102*, 6467–6493, 1997.

Miyoshi, A., S. Hatakeyama, and N. Washida, OH radical-initiated photooxidation of isoprene: An estimate of global CO production, *J. Geophys. Res.*, *99*, 18,779–18,787, 1994.

Niki, H., and P. D. Maker, Atmospheric Reactions Involving Hydrocarbons: Long path-FTIR studies, in *Advances in Photochemistry*, edited by D. H. Volman, G. S. Hammond, and K. Gollnick, p. 69, John Wiley, New York, 1990.

Ohta, T., Furan ring formation in OH-initiated photooxidation of 1,3-butadiene and *cis*-1,3-pentadiene, *Bull. Chem. Soc. Jpn.*, *57*, 960–966, 1984.

Paulson, S. E., and J. H. Seinfeld, Development and evaluation of a photooxidation mechanism for isoprene, *J. Geophys. Res.*, *97*, 20,703–20,715, 1992.

Paulson, S. E., R. C. Flagan, and J. H. Seinfeld, Atmospheric photooxidation of isoprene, part I, The hydroxyl radical and ground state atomic oxygen reactions, *Int. J. Chem. Kinet.*, *24*(1), 79–101, 1992.

Platz, J., J. Sehested, O. Nielsen, and T. Wallington, Atmospheric chemistry of cyclohexane: UV spectra of c-C6H11 and (c-C6H11)O-2 radicals, kinetics of the reactions of (c-C6H11)O-2 radicals with NO and NO2, and the fate of the alkoxy radical (c-C6H11)O, *J. Phys. Chem. A*, *103*(15), 2688–2695, 1999.

Poisson, N., M. Kanakidou, and P. J. Crutzen, Impact of non-methane hydrocarbons on tropospheric chemistry and the oxidizing power of the global troposphere: 3-dimensional modelling results, *J. Atmos. Chem.*, *36*(2), 157–230, 2000.

Rothman, L. S., et al., The 1996 HITRAN molecular spectroscopic database and HAWKS (HITRAN atmospheric workstation), *J. Quant. Spectrosc. Radiat. Transfer*, *60*(5), 665–710, 1998.

Ruppert, L., and K. H. Becker, A product study of the OH radical-initiated oxidation of isoprene: Formation of C5-unsaturated diols, *Atmos. Environ.*, *34*(10), 1529–1542, 2000.

Starn, T. K., P. B. Shepson, S. B. Bertman, J. S. White, B. G. Splawn, D. D. Riemer, R. G. Zika, and K. Olszyna, Observations of isoprene chemistry and its role in ozone production at a semirural site during the 1995 Southern Oxidants Study, *J. Geophys. Res.*, *103*, 22,425–22,435, 1998.

Stevens, P. S., et al., HO_2/OH and RO_2/HO_2 ratios during the Tropospheric OH Photochemistry Experiment: Measurement and theory, *J. Geophys. Res.*, *102*, 6379–6391, 1997.

Stevens, P., L. Esperance, B. Chuong, and G. Martin, Measurements of the kinetics of the OH–initiated oxidation of isoprene: Radical propagation in the OH + isoprene + O_2 + NO reaction system, *Int. J. Chem. Kinet.*, *31*, 637–643, 1999.

Stevens, P. S., E. Seymour, and Z. Li, Theoretical and experimental studies of the reaction of OH with isoprene, *J. Phys. Chem. A*, *104*, 5989–5997, 2000.

Tuazon, E. C., and R. Atkinson, A product study of the gas-phase reaction of methyl vinyl ketone with the OH radical in the presence of NOx, *Int. J. Chem. Kinet.*, *21*(12), 1141–1152, 1989.

Tuazon, E. C., and R. Atkinson, Product study of the gas-phase reaction of isoprene with the OH radical in the presence of NOx, *Int. J. Chem. Kinet.*, *22*(12), 1221–1236, 1990a.

Tuazon, E. C., and R. Atkinson, A product study of the gas-phase reaction of methacrolein with the OH radical in the presence of NOx, *Int. J. Chem. Kinet.*, *22*(6), 591–602, 1990b.

Tuazon, E. C., A. Alvarado, S. M. Aschmann, R. Atkinson, and J. Arey, Products of the gas-phase reactions of 1,3-butadiene with OH and NO_3 radicals, *Environ. Sci. Technol.*, *33*(20), 3586–3595, 1999.

U.S. Department of Health and Human Services, *Ninth Report on Carcinogens, 1,3-butadiene*, p. III-14, 2001.

Yu, J., H. E. Jeffries, and R. M. Le Lacheur, Identifying airborne carbonyl compounds in isoprene atmospheric photooxidation products by their PFBHA oximes using gas chromatography/ion trap mass spectrometry, *Environ. Sci. Technol.*, *29*(8), 1923–1932, 1995.

Zhang, R., I. Suh, W. Lei, A. D. Clinkenbeard, and S. W. North, Kinetic studies of OH-initiated reactions of isoprene, *J. Geophys. Res.*, *105*, 24,627–24,635, 2000.

J. G. Anderson, Department of Chemistry and Chemical Biology, Harvard University, 40 Oxford Street, Cambridge, MA 02138, USA. (james_anderson@huarp.harvard.edu)

K. L. Demerjian and M. Sprengnether, Atmospheric Sciences Research Center, State University of New York at Albany, 100 Fuller Road, Albany, NY 12205, USA. (kld@asrc.cestm.albany.edu; sprengnether@huarp.harvard.edu)

N. M. Donahue, Carnegie Mellon University, Pittsburgh, Pennsylvania, USA. (Nmd+@cmu.edu)